Acta Crystallographica Section D
Biological Crystallography
ISSN 0907-4449

Reindeer β-lactoglobulin crystal structure with pseudo-body-centred noncrystallographic symmetry

Esko Oksanen,[a] Veli-Pekka Jaakola,[a] Tiina Tolonen,[b] Kaija Valkonen,[b] Bo Åkerström,[c] Nisse Kalkkinen,[a] Vesa Virtanen[b] and Adrian Goldman[a]*

[a]Institute of Biotechnology, University of Helsinki, Finland, [b]Laboratory of Biotechnology, University of Oulu, Finland, and [c]Department of Clinical Sciences, Lund University, Sweden

Correspondence e-mail: adrian.goldman@helsinki.fi

Received 10 January 2006
Accepted 10 August 2006

PDB Reference: reindeer β-lactoglobulin, 1yup, r1yupsf.

Reindeer β-lactoglobulin (βLG) belongs to the lipocalin superfamily. Its DNA and protein sequences have been determined and showed that it had nine residue changes from bovine βLG. Reindeer βLG, the structure of which was finally determined at 2.1 Å resolution in space group $P1$, crystallized in a unit cell that is both $P2$-like and $P2_1$-like owing to the presence of an almost perfect (but noncrystallographic) body-centring vector. The non-body-centred data could only be observed using a very bright synchrotron beam and a novel refinement strategy was adopted to enable us to use the weak $h + k + l = 2n + 1$ reflections.

1. Introduction

β-Lactoglobulin (βLG) is an abundant whey protein present in the milk of many, although not all, mammals. β-Lactoglobulins belong to the lipocalin superfamily (Åkerström *et al.*, 2000). Lipocalins share an eight-stranded antiparallel β-barrel fold with one α-helix, despite low sequence homology within the superfamily (Flower, 2000). The most extensively studied lipocalin is bovine β-lactoglobulin. Despite investigations by a large number of biochemical and biophysical techniques, its biological function remains to be established (Sawyer & Kontopidis, 2000).

However, β-lactoglobulin is known to bind hydrophobic molecules such as retinol or palmitic acid in a calyx in the centre of the β-barrel. The protein is also very acid-stable, even in the conditions of the stomach (Sakai *et al.*, 2000). Bovine βLG was first purified and crystallized in 1934 (Palmer, 1934) and a crystal structure was solved at 6 Å in 1979 (Green *et al.*, 1979). The first high-resolution X-ray structure of βLG at 1.8 Å resolution was solved in 1996 (Brownlow *et al.*, 1997).

Unlike bovine βLG, there are no genetic variants of reindeer βLG (Rytkönen *et al.*, 2002). The differences between bovine and reindeer βLG at the levels of sequence and structure were unknown. In order to identify these differences, we have determined the partial DNA and protein sequences of reindeer βLG, crystallized it in two different forms and determined the crystal structure. The structure determination was seriously complicated by the presence of translational pseudosymmetry.

2. Materials and methods

2.1. Protein purification and DNA sequencing

Reindeer (*Rangifer tarandus*) β-lactoglobulin was purified from reindeer milk as described elsewhere (Heikura *et al.*, 2005). The molecular mass of the purified protein was deter-

Table 1
Data-collection and processing statistics.

Values in parentheses are for the highest resolution shell.

Space group	*P*1	*P*2†
Unit-cell parameters (Å, °)	a = 52.24, b = 94.14, c = 64.15, α = 90, β = 105.8, γ = 90	a = 52.20, b = 94.10, c = 64.20, α = 90, β = 105.7, γ = 90
Wavelength (Å)	1.73114	1.73114
Resolution (Å)	20–2.1 (2.23–2.1)	20–2.1 (2.23–2.1)
Unique reflections	63793 (9725)	33437 (5176)
Completeness (%)	91.6 (86.2)	95.8 (92.5)
$R_{\rm sym}$‡	7.0 (22.7)	8.1 (28.1)
$\langle I/\sigma(I)\rangle$	6.6 (2.5)	14.0 (5.0)
Redundancy	3.2 (3.1)	6.2 (6.0)
Solvent content (%)	48.6	48.6
Monomers per ASU	8	4

† The statistics in *P*2 and $P2_1$ are equivalent. ‡ $R_{\rm sym} = \sum_{hkl}|I(hkl) - \langle I(hkl)\rangle|/\sum_{hkl}(hkl)$, where $\langle I(hkl)\rangle$ is the mean of the symmetry-equivalent reflections of $I(hkl)$.

Table 2
Final refinement statistics.

The refinement was only carried out in *P*1 (see text for details). Values in parentheses are for the highest resolution shell.

Total unique reflections	63710
Reflections in test set (5%)	3186
$R_{\rm work}$†	0.235 (0.353)
$R_{\rm free}$‡	0.311 (0.401)
No. of atoms used in refinement	10045
No. of water molecules	361
Average *B* factor (all atoms) (Å^2)	36.7
Bond-length r.m.s.d. from ideality (Å)	0.014
Bond-angle r.m.s.d. from ideality (°)	1.558
Ramachandran plot	
Residues in most favoured regions (%)	84.3
Residues in additionally allowed regions (%)	12.9
Residues in generously allowed regions (%)	1.0
Residues in disallowed regions (%)	1.7

† $R_{\rm work} = \sum_{hkl}[|F_{\rm o}(hkl)| - |F_{\rm c}(hkl)|]/\sum_{hkl}|F_{\rm o}(hkl)|$ for $F(hkl)$ not belonging to the test set. ‡ $R_{\rm free} = \sum_{hkl}[|F_{\rm o}(hkl)| - |F_{\rm c}(hkl)|]/\sum_{hkl}|F_{\rm o}(hkl)|$ for $F(hkl)$ in the test set.

mined by electrospray mass spectrometry using a Q-TOF instrument (Micromass Ltd, Manchester, England) directly and after alkylation with 4-vinylpyridine. MALDI–TOF mass spectrometry (Ultralex TOF/TOF, Bruker-Daltonik GmbH, Bremen, Germany) and N-terminal sequencing of the protein and its internal peptides after endoproteinase cleavage were performed as described elsewhere (Ylönen *et al.*, 1999). Genomic DNA was isolated (Miller *et al.*, 1988) from reindeer whole blood samples (obtained from the Finnish Game and Fisheries Research Institute, Reindeer Research Station, Kaamanen, Finland). The coding sequences and 5′- and 3′-flanking noncoding sequences of reindeer βLG were determined by PCR using specific intron primers based on bovine (Z48305) and ovine (X12817) gene sequences obtained from GenBank (Innis *et al.*, 1990). Purified PCR products were then sequenced at the Division of Transfusion Medicine, Lund University, Lund, Sweden and the Department of Medical Biochemistry and Molecular Biology, University of Oulu, Finland.

2.2. Crystallization and structure solution

Reindeer βLG was first crystallized from 0.1 *M* MES pH 6.0, 30% PEG MME 550 and 0.01 *M* zinc sulfate. The space group was $P4_1$ and the crystals diffracted to 3.2 Å resolution at ESRF beamline ID14-3, but owing to perfect hemihedral twinning the structure could not be refined. We therefore rescreened and identified a new crystal form from a sodium malonate screen. Crystals were grown from sitting drops composed of 4 µl 17 mg ml^{-1} protein solution (in 20 m*M* sodium/potassium phosphate buffer pH 7.4) and 4 µl reservoir solution consisting of 2.6 *M* sodium malonate pH 6.5. The reservoir volume was 700 µl. Crystals were grown at 277 K and appeared in one or two weeks. They typically grew to 0.05 × 0.05 mm. Data were collected at ESRF beamline ID29 at 100 K and were processed with the program *XDS* (Kabsch, 1993) in space groups *P*1, *P*2 and $P2_1$ (Table 1), for reasons which will be explained below. Structure solution and refinement were performed with the *CCP*4 program suite (Collaborative Computational Project, Number 4, 1994). The structure was solved by molecular replacement with *MOLREP* (Vagin & Teplyakov, 1997) and refined with *REFMAC*5 (Murshudov *et al.*, 1997). Individual isotropic *B* factors were refined in restrained refinements and overall isotropic *B* factors in rigid-body refinements. The structure of bovine βLG at pH 6 (PDB code 1beb) was used as a molecular-replacement model. Manual model building was performed in *O* (Jones *et al.*, 1991) and the model was validated with *PROCHECK* (Laskowski *et al.*, 1993; Table 2). The structure-factor amplitude ratios were calculated with *DATAMAN* (Kleywegt & Jones, 1996).

2.3. Analysis of the crystal symmetry

The data were initially indexed in a primitive monoclinic lattice and systematic absences along b^* suggested that the space group would be $P2_1$. A clear molecular-replacement solution could be obtained in $P2_1$ using either a monomer or a dimer model, but refinement was unsuccessful. Both solutions had four monomers in the asymmetric unit and the dimer interface of bovine βLG was accurately reproduced with the monomer model. A notable feature of this structure solution was that the crystallographic twofold screw axis ran through the monomer, which is highly unlikely. Surprisingly enough, a molecular-replacement solution could also be found in space group *P*2. This solution was related to that in $P2_1$ by a translation vector (0.25, 0.0, 0.25) in fractional coordinates. Owing to this quarter unit-cell shift, the crystallographic twofold axis was placed between monomers and refinement again attempted. This solution also could not be refined, so a lower symmetry space group was chosen. A molecular-replacement solution in *P*1 using a monomeric model had eight monomers in the asymmetric unit and also reproduced the dimer interface as above. The native Patterson map showed a strong peak exactly at (0.5, 0.5, 0.5) in fractional coordinates. This 60σ peak was 43%, not 100%, of the origin peak, indicating that the peak was not a crystallographic centring vector but a noncrystallographic centring vector. The

self-rotation function calculated in $P1$ (Fig. 1) indicates a twofold along b and another twofold which we found related the two monomers within a dimer. From this element, the twofold along b also generates a third twofold. The peak in the Patterson synthesis indicates the presence of a noncrystallographic body-centring operation. Such an operation is expected to cause the intensity of the $h + k + l = 2n + 1$ ('odd') reflections to be much weaker than the intensity of the $h + k + l = 2n$ ('even') reflections. This is indeed observed, as summarized in Table 3. Another indication that the body-centring vector is non-crystallographic is that the associated reflection condition $h + k + l = 2n$ is only observed at low resolution (Fig. 2); at high resolution the intensity of the 'odd' reflections and 'even' reflections are about the same (Table 3).

Table 3
Structure-factor amplitude ratios for reflections with $h + k + l$ odd or even.

Resolution range (Å)	No. of reflections with $h + k + l = 2n + 1$	No. of reflections with $h + k + l = 2n$	$\langle\lvert F\rvert_{\rm odd}\rangle/\langle\lvert F\rvert_{\rm even}\rangle$
20–2.1	31922	31788	0.397
20–3.5	7175	7007	0.274
20–3.0	11317	11174	0.319
3.0–2.1	20605	20614	0.813
2.5–2.1	12612	12550	0.990

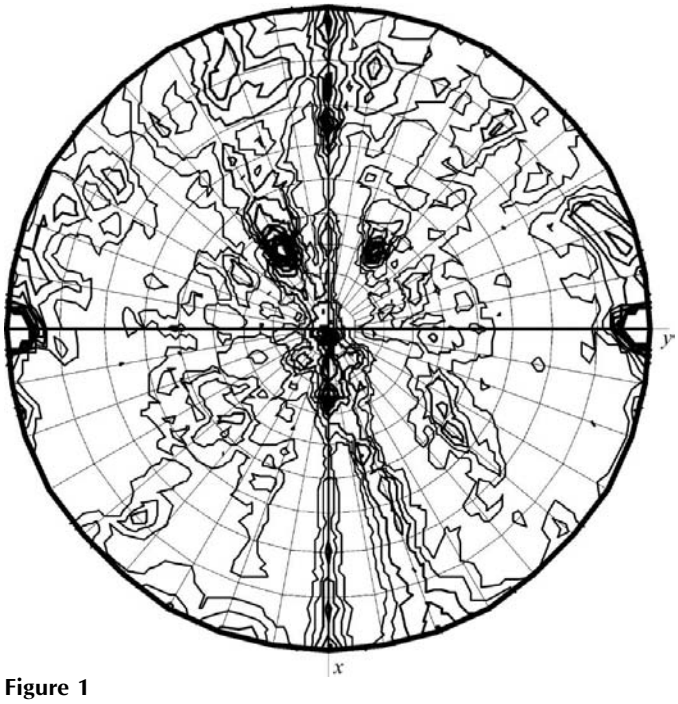

Figure 1
Self-rotation function ($\chi = 180^\circ$) calculated in space group $P1$, showing the twofold along the b axis and the approximate twofold between two monomers in a dimer.

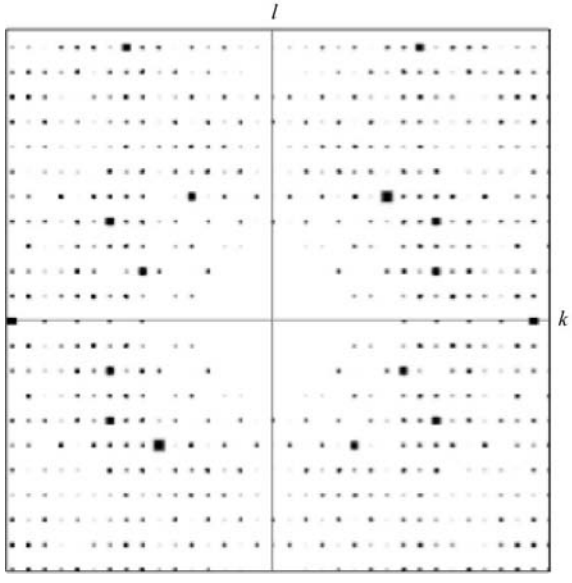

Figure 2
Pseudo-precession photograph showing the pattern of strong and weak reflections on the (0kl) plane of reciprocal space.

A data set collected on our home source to 2.5 Å resolution could not be indexed in a primitive monoclinic lattice. Instead, a C-centred monoclinic lattice ($a = 71.30$, $b = 95.50$, $c = 53.00$ Å, $\beta = 119.60^\circ$) corresponding to perfect body-centring was found. Since the systematically weak reflections were not observed, the problem could not be diagnosed from the home-collected data. The space-group ambiguity results from the pseudocentrin: a non-crystallographic centring vector generates an NCS twofold from a crystallographic twofold screw and *vice versa*. Translational pseudosymmetry complicates crystallographic refinement significantly, since the assumption that the intensities of reflections are independent is no longer valid. This leads to crystallographic R values that are significantly higher than those normally expected for a correct structure (Wilson, 1950). Maximum-likelihood refinement also assumes independent data (McCoy, 2004). Although this is an approximation in all macromolecular refinements (Pannu & Read, 1996), the correlations are particularly strong when pseudosymmetry is present. Nonetheless, two protein structures with translational pseudosymmetry have been solved (Poy *et al.*, 2001; Vajdos *et al.*, 1997).

As a large number of reflections were very weak, the estimation of the error of these reflections (although particularly challenging) is very important, because the weak $h + k + l = 2n + 1$ reflections contain all the information about the precise position of the monomers in the unit cell and any differences between them. For this reason the $(h + k + l)$ = odd and even reflections were scaled separately, so as to be able to obtain proper estimates of their intensities and standard deviations. The cumulative intensity distribution of both sets resembled the expected distribution. Rigid-body refinement against the $(h + k + l)$ = odd data was performed to establish the positions of the monomers, followed by restrained refinement against the $(h + k + l)$ = even data. After a few such cycles, the model was refined against all data. Even though the procedure is somewhat *ad hoc*, it reduced the R values considerably. The R values changed as described below; the R values are higher for the $(h + k + l)$ = odd data, since these data are much weaker and hence less accurate.

After molecular replacement with a monomer model the R value was 0.567 against all data. 20 cycles of rigid-body

refinement against the $(h + k + l)$ = odd data lowered R/R_{free} to 0.425/0.434. Subsequent restrained refinement against the $(h + k + l)$ = even data resulted in R/R_{free} of 0.281/0.350. A second rigid-body refinement against the $(h + k + l)$ = odd data lowered the R/R_{free} from 0.406/0.411 to 0.385/0.400. The starting R values against the $(h + k + l)$ data were lower than in the previous rigid-body refinement because the model was improved by refinement against the $(h + k + l)$ = even data. The R/R_{free} of this model against all data was 0.412/0.414, which decreased to 0.304/0.358 upon restrained refinement. Refinement and manual model building against all data improved the model and maps; nonetheless, the R values remained quite high (R/R_{free} = 0.235/0.311; Table 2) because of the large number of $|F_{obs}|$s with very low but non-zero values. The overall quality of the electron-density maps was nonetheless reasonably good (Fig. 3) and allowed us to see differences between the monomers in the asymmetric unit.

3. Results

3.1. Sequence data

Reindeer β-lactoglobulin, which is very similar to the bovine protein, differing by only nine residues out of 162, is an 18 kDa protein that also exists as a dimer at physiological pH. Since the biological function is not known (Sawyer & Kontopidis, 2000), it can only be assumed that the functional form is also a dimer. Electrospray mass-spectrometric analysis of reduced 4-vinylpyridine-alkylated (a theoretical addition of 105.14 mass units to each cysteine residue) βLG gave a molecular mass of 18 802.0, which corresponds to a molecular mass of 18 276.2 for the nonderivatized polypeptide chain. This agrees with the suggested protein sequence. The non-alkylated protein gave a molecular mass of 18 272.0, as determined by electrospray mass spectrometry, which indicates the presence of two disulfide bridges in the monomer protein. The correctness of the amino-acid sequence used for reindeer βLG was further verified by N-terminal sequencing of the protein (43 residues) combined with analysis of its proteolytic fragments by MALDI–TOF mass fingerprinting and direct sequence analysis of selected peptides. Comparison with the previously reported bovine (Z48305) and ovine (X12817) βLG gene sequences demonstrates that the reindeer sequences (GenBank DQ055845, DQ055846, DQ055847, DQ055848, DQ055849, DQ055850) reported here contain the seven exon sequences and parts of the intron sequence of the reindeer βLG gene. The analysed DNA sequences are also in agreement with the suggested protein sequence.

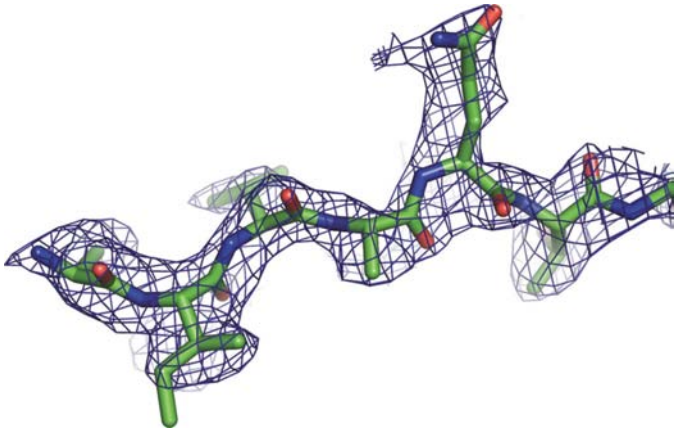

Figure 3
The extended conformation of the N-terminus, showing a σ_A-weighted $2F_o - F_c$ electron-density map contoured at 1σ.

3.2. Structural data

The structure of reindeer βLG is nearly identical to the bovine βLG structure at pH 6 (Fig. 4). The root-mean-square deviation is 0.45 Å per C^{α} atom for residues 10–160. We found a total of 20 residues in disallowed conformations in the Ramachandran plot (Table 2). Of these, Ala34, Asn63 and Tyr99 occur in disallowed regions in bovine as well as reindeer βLG (Brownlow *et al.*, 1997). Indeed, Tyr93 is part of a conserved γ-turn characteristic of the lipocalin superfamily (Brownlow *et al.*, 1997). The others (Asn5, Asn159 and Cys160) are at the termini, which are somewhat poorly defined. The side-chain conformations also show very few differences from the bovine protein. The sequence differences are located in residues that are exposed to the solvent. As a result of this, the charge distribution on the surface of the reindeer protein is significantly different from that of the bovine protein. This partly explains the differences in solubility and crystal packing. The residues lining the hydrophobic calyx have practically identical conformations and the EF-loop is in the closed conformation, blocking access to the calyx, which in this structure is empty.

Figure 4
The C^{α} traces of bovine βLG at pH 6.0 (red) and at pH 7.5 complexed with palmitate (green) superposed on reindeer βLG (blue). The conformation of reindeer βLG is almost identical to that of bovine βLG with no bound ligand. The bound palmitate is shown in green.

The asymmetric unit contains eight monomers. They are arranged in four dimers (*AB*, *CD*, *EF* and *GH*), each identical to the bovine βLG dimer at pH 6. The pairs of dimers *AB* + *CD* and *EF* + *GH* are related by a twofold axis along *b*, so in *P*2 or $P2_1$ only one such pair would be present. The packing of these dimers gives rise to the unusual translational pseudosymmetry relating one dimer to another by a translation vector of approximately (0.5, 0.5, 0.5) in fractional coordinates (Fig. 5). The vector is somewhat different between the pairs of dimers, as summarized in Table 4. This is also observed in the Patterson map as an elongation of the peak in the $u = w$ direction.

The differences between the NCS-related monomers are very slight, with root-mean-square deviations per C^{α} atom of ~0.3 Å between monomers. In some of the monomers the N- and C-termini are also visible, unlike the bovine structures. In chain *A*, all residues from 1 to 162 are visible, but the N-terminus is not visible in the electron density in chains *E* and *H*, possibly owing to inaccuracies in the positions of the monomers. The N-terminus is in an extended conformation (Fig. 3). The conformation of the C-terminus varies slightly between the NCS-related monomers, with the two last residues only visible in some monomers. The disulfide bridges Cys66–Cys160 and Cys109–Cys119 are formed as in bovine βLG.

Table 4
Summary of translation vectors in fractional coordinates.

Translation	*x*	*y*	*z*	R.m.s.d. (Å)
AB→*CD*	0.51	0.47	0.54	0.330
EF→*GH*	0.49	0.49	0.46	0.332
A→*C*	0.50	0.49	0.50	0.287
B→*D*	0.50	0.49	0.50	0.254
E→*G*	0.48	0.50	0.45	0.270
F→*H*	0.50	0.50	0.40	0.261

4. Discussion

As the high sequence homology suggests, the structures of bovine and reindeer βLG are very similar. Since the differences occur in surface residues, the properties of the protein are altered. This is demonstrated both by the lower solubility of reindeer βLG, presumably owing to differing charge distributions on the surface, and the different crystal forms of the two proteins. The symmetry of the crystal is rather unusual, being apparently consistent with both *P*2 and $P2_1$ space groups. Pseudocentring in protein crystals has been reported in the literature (Chook *et al.*, 1998), but the occurrence of such pseudosymmetry may be more frequent than the literature suggests, since the data is likely to be indexed in an incorrect centred space group. This leads to the exclusion of the pseudo-absent reflections from the integration step, making it very difficult to diagnose the problem. In the case of reindeer βLG, the extremely bright X-ray beam from a synchrotron source was crucial for observing the weak reflections. The robust spot-finding algorithm of the data-processing software and the use of all the spots in indexing were also critical. Using only the strongest reflections in indexing will lead to a failure to detect pseudosymmetry of this kind and the subsequent refinement will fail. Consequently, crystals exhibiting translational pseudosymmetry can easily be left unsolved and unpublished, simply because the problem cannot be identified.

A crystal with a pseudotranslation can be considered as a sum of a superstructure, namely the positions of the monomers, and a substructure, which is the structure of the individual monomer (Cascarano *et al.*, 1985). The reflections can be divided into superstructure and substructure reflections, which should be treated separately; there currently is no macromolecular crystallographic refinement package where this can be performed correctly, nor, indeed, any in which it can be performed except as an *ad hoc* procedure as performed here.

We tried a number of different strategies to improve the structure solution. Among them were using different molecular-replacement programs, such as *CNS*, *BEAST* or *Phaser*, tracing the molecule with *ARP*/*wARP*, simulated annealing, performing rigid-body refinement with various different rigid groups or NCS-phased refinement. None of these were better than the approach described in §2.3. Lowering the resolution during the early stages of refinement also did not help. Why? As shown (Fig. 4) there is essentially no difference between bovine and reindeer βLG; this is essentially a point-mutant structure. The *R* factors for such refinements usually 'drop like a stone' once the molecular-replacement solution has been found. In this case it did not because the problem lies not in the monomer structure but in the pseudosymmetry: their overall positioning in the unit cell. In other words, the problems result from indeterminacy arising from refining against reflections very close to zero. Worse still, as only the

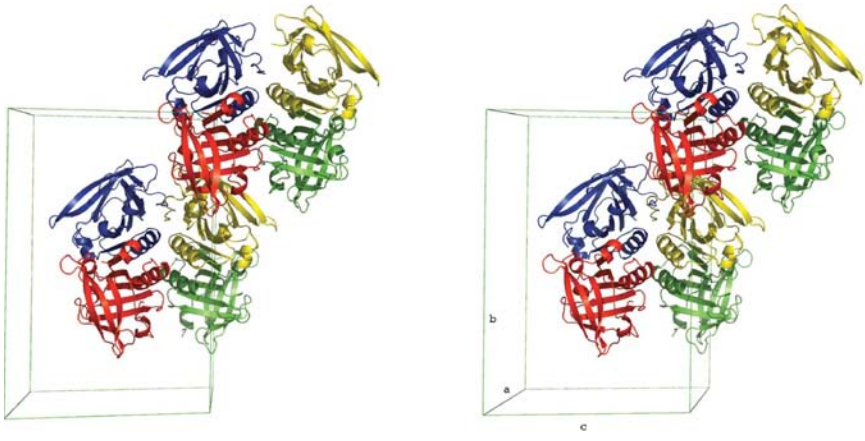

Figure 5
A stereo figure of the pairs of dimers in the asymmetric unit related by the pseudo-translation vector. The monomers are related by a vector along the body diagonal of the unit cell. Each monomer and its pseudosymmetry mate are shown in the same colour. The unit cell is shown in green.

systematically weak ($h + k + l$) = odd reflections determine the position of the monomers, using only the low-resolution reflections would be fruitless as they are even weaker, leading to even less well defined positioning of the molecules.

Summa summarum, the difficulties in refinement were caused by the uncertainty in the monomer positions (superstructure), not in the structure of the individual monomers (substructure). For such cases, maximum-likelihood functions for refinement could and should be adjusted to deal with pseudosymmetry. In the meantime, the *ad hoc* procedure we describe here has worked well in a case with pseudosymmetry even higher than those reported by Chook *et al.* (1998).

The authors wish to thank Seija Mäki for help with crystallization, Lari Lehtiö for help with computers and crystallography and the ESRF beamline staff for assistance with data collection. The work was funded by Tekes (grant No. 460457), Biocentrum Helsinki and the Academy of Finland (grant No. 1105157) and the Informational and Structural Biology graduate school. The work of TT was supported by the mobility scholarship of NordForsk, Nordic Research Board (reference No. 040137) and Sotkamo municipality. TT wishes to thank Jill Storry from the Division of Transfusion Medicine, Lund University, Lund, Sweden for help and advice concerning DNA sequencing. Reindeer blood was obtained from Mauri Nieminen (PhD). Beamtime was made available under the European Union Improving Human Potential Programme (Access to Research Infrastructures) at the ESRF under contract No. HPRI-CT-1999-00022.

References

Åkerström, B., Flower, D. R. & Salier, J. P. (2000). *Biochim. Biophys. Acta*, **1482**, 1–8.
Brownlow, S., Morais Cabral, J. H., Cooper, R., Flower, D. R., Yewdall, S. J., Polikarpov, I., North, A. C. & Sawyer, L. (1997). *Structure*, **5**, 481–495.
Cascarano, G., Giacovazzo, C. & Luic, M. (1985). *Acta Cryst.* A**41**, 544–551.
Chook, Y. M., Lipscomb, W. N. & Ke, H. (1998). *Acta Cryst.* D**54**, 822–827.
Collaborative Computational Project, Number 4 (1994). *Acta Cryst.* D**50**, 760–763.
Flower, D. R. (2000). *Biochim. Biophys. Acta*, **1482**, 46–56.
Green, D. W., Aschaffenburg, R., Camerman, A., Coppola, J. C., Dunnill, P., Simmons, R. M., Komorowski, E. S., Sawyer, L., Turner, E. M. & Woods, K. F. (1979). *J. Mol. Biol.* **131**, 375–397.
Heikura, J., Suutari, T., Rytkönen, J., Nieminen, M., Virtanen, V. & Valkonen, K. (2005). *Milchwissenschaft*, **60**, 388–392.
Innis, M. A., Gelfand, D. H., Sninsky, J. J. & White, T. J. (1990). *PCR Protocols: A Guide to Methods and Applications.* San Diego: Academic Press.
Jones, T. A., Zou, J.-Y., Cowan, S. W. & Kjeldgaard, M. (1991). *Acta Cryst.* A**47**, 110–119.
Kabsch, W. (1993). *J. Appl. Cryst.* **26**, 795–800.
Kleywegt, G. J. & Jones, T. A. (1996). *Acta Cryst.* D**52**, 826–828.
Laskowski, R. A., MacArthur, M. W., Moss, D. S. & Thornton, J. M. (1993). *J. Appl. Cryst.* **26**, 283–291.
McCoy, A. J. (2004). *Acta Cryst.* D**60**, 2169–2183.
Miller, S. A., Dykes, D. D. & Polesky, H. F. (1988). *Nucleic Acids Res.* **16**, 1215.
Murshudov, G. N., Vagin, A. A. & Dodson, E. J. (1997). *Acta Cryst.* D**53**, 240–255.
Palmer, A. H. (1934). *J. Biol. Chem.* **104**, 359–372.
Pannu, N. S. & Read, R. J. (1996). *Acta Cryst.* A**52**, 659–668.
Poy, F., Lepourcelet, M., Shivdasani, R. A. & Eck, M. J. (2001). *Nature Struct. Biol.* **8**, 1053–1057.
Rytkönen, J., Alatossava, T., Nieminen, M. & Valkonen, K. (2002). *Milchwissenschaft*, **57**, 259–261.
Sakai, K., Sakurai, K., Sakai, M., Hoshino, M. & Goto, Y. (2000). *Protein Sci.* **9**, 1719–1729.
Sawyer, L. & Kontopidis, G. (2000). *Biochim. Biophys. Acta*, **1482**, 136–148.
Vagin, A. & Teplyakov, A. (1997). *J. Appl. Cryst.* **30**, 1022–1025.
Vajdos, F. F., Yoo, S., Houseweart, M., Sundquist, W. I. & Hill, C. P. (1997). *Protein Sci.* **6**, 2297–2307.
Wilson, A. (1950). *Acta Cryst.* **3**, 397–398.
Ylönen, A., Rinne, A., Herttuainen, J., Bogwald, J., Järvinen, M. & Kalkkinen, N. (1999). *Eur. J. Biochem.* **266**, 1066–1072.